Biomaterials Science

ROYAL SOCIETY OF CHEMISTRY

PAPER

View Article Online
View Journal | View Issue

Cite this: *Biomater. Sci.*, 2020, **8**, 2514

Assembly of FN-silk with laminin-521 to integrate hPSCs into a three-dimensional culture for neural differentiation†

Carolina Åstrand,[a,b] Veronique Chotteau,[c,d] Anna Falk[e] and My Hedhammar *[a]

Three-dimensional (3D) neural tissue cultures recapitulate the basic concepts during development and disease better than what can be obtained using conventional two-dimensional cultures. Here, we use a recombinant spider silk protein functionalized with a cell binding motif from fibronectin (FN-silk) in combination with a human recombinant laminin 521 (LN-521) to create a fully defined stem cell niche in 3D. A novel method to assemble silk blended with LN-521 together with human pluripotent stem cells (hPSC) is used to create centimeter-sized foams, which upon cultivation develop into 3D cell constructs supported by a microfibrillar network. After initial cell expansion, neural differentiation was induced to form a homogenous layer of continuous neuroectodermal tissue that allows further differentiation into neuronal subtypes. The silk-supported 3D cell constructs could then be detached from the bottom of the well and cultured as floating entities, where cells appeared in distinctive radial organization resembling early neural tube. This shows that the neural progenitors retain their cellular self-organization ability in the FN-silk/LN-521-supported 3D culture. Calcium imaging demonstrated spontaneous activity, which is important for the formation of neuronal networks. Together, the results show that hPSCs integrated into FN-silk/LN-521 foam develop into neural progenitors and that these stay viable during long-term differentiations. FN-silk/LN-521 also supports morphogenesis mimicking the human brain development and can serve as base for engineering of hPSC-derived neural tissue.

Received 9th October 2019,
Accepted 14th March 2020

DOI: 10.1039/c9bm01624d

rsc.li/biomaterials-science

1. Introduction

Human pluripotent stem (hPSC) cells, including human embryonic stem cells (hESC) and human induced pluripotent stem cells (hiPS), have the ability to generate any specialized cell in the body. hPSCs have been used for engineering of a wide variety of human tissue, including models of neurogenesis.[1] Three-dimensional (3D) cultures formed by self-organization of hPSCs have been able to partly recapitulate the cellular organization of cortical-,[2] retinal-,[3] and cerebral tissue.[4] Such 3D cultures are currently used for studying human brain development, function and disease. They are also explored for drug screening purposes and for the development of cell replacement therapies.[1] Recent advances to differentiate spheroid-based hPSC cultures into cerebral organoids[4] have given new insights in neural disease by *e.g.* modelling of the exposure of Zika virus to the fetal brain[5] and autism spectrum disorders.[6] An approach to expand the organoid culture to generate laminated slices mimicking cortex-like structures has also been reported.[7] However, these systems that are largely based on intrinsic cellular self-organization share limitations such as; (i) little control of the cell type fates, (ii) low reproducibility and (iii) difficulty to scale up.[8]

In contrast to culture systems based on cellular self-assembly, methods using supporting scaffolds/matrices generally give a higher degree of control of the microenvironment.[9] Several criteria have to be fulfilled for a matrix to be able to support the important extrinsic signals that regulate cell behavior. Primarily, the chemical composition and morphology of the matrix have to support hPSC attachment and promote survival.[10] Neural progenitors have been grown on matrices made of a range of proteins such as collagen, fibrin, fibronectin and laminin,[11] but of these only a few have the ability to also support pluripotent cells. Any ill-defined components

[a]*Dept. of Protein Science, School of Engineering Sciences in Chemistry, Biotechnology and Health, KTH-Royal Institute of Technology, SE-10691 Stockholm, Sweden. E-mail: myh@kth.se*
[b]*Spiber Technology AB, Stockholm, Sweden*
[c]*Dept. of Industrial Biotechnology, School of Engineering Sciences in Chemistry, Biotechnology and Health, KTH-Royal Institute of Technology, SE-10691 Stockholm, Sweden*
[d]*AdBIOPRO Competence Centre for Advanced BioProduction by Continuous Processing, Sweden*
[e]*Dept. of Neuroscience, Karolinska Institutet, SE-17177 Stockholm, Sweden*
†Electronic supplementary information (ESI) available. See DOI: 10.1039/c9bm01624d

reduce predictability and reproducibility of tissue organization.[12] Recently, a hybrid hydrogel with natural (gelatin) and synthetic (PEG) components were shown to stimulate cell differentiation (in this case mesenchymal stem cells).[13] Permeability of the matrix is crucial to allow exchange of nutrients and waste products. Furthermore, the stiffness of the material is known to be important for cellular behavior.[14] By screening synthetic matrices for a variety of mechanical and biochemical properties it was seen that the matrix surrounding the cells affected cell orientation during neural tube formation.[15] In line with this, synthetic microfilaments have been shown able to aid the organization of cells into a cortical plate.[12]

Due to its favorable mechanical properties and biocompatibility, silk spun by spiders have successfully been used for peripheral nerve regeneration.[16,17] Pre-made scaffolds of recombinant spider silk protein have been shown to support neural stem cell culture.[18] Furthermore, silk scaffolds combined with gels consisting of extracellular matrix proteins have been used for mimicking the modularity of cortical tissue.[19] The recombinant spider silk protein 4RepCT has previously been functionalized with cell binding motifs from fibronectin (FN-silk)[20] and vitronectin (VN-silk).[21] A coating of VN-silk was shown able to support long-term expansion of hPSCs grown as monolayers[22] and premade scaffolds of VN-silk could serve as a substrate supporting differentiation into neuroectoderm.[21] FN-silk has been found to promote attachment and proliferation of human primary cells.[20] We recently reported that the FN-silk protein can assemble in the presence of cells under physiological-like conditions into a 3D network of microfibers, rendering evenly distributed cells.[23]

In this study, we investigated how FN-silk can be used to create a 3D culture system suitable for expansion of hPSCs and following neural differentiation. Recombinant human laminin 521 (LN-521) has been shown advantageous in promoting self-renewal and pluripotency of hPSCs.[24] It has also been shown beneficial to combine recombinant laminins with other matrices (fibrin gels) to promote expansion of cells (epithelial progenitor).[25] Therefore, we herein investigated the option to combine FN-silk, which enables self-assembly into a 3D environment, with LN-521, which offers biologically relevant cues for the sensitive hPSCs. The method allows integration of hPSCs into an extracellular matrix-like microfibrillar network of fully defined FN-silk/LN-521. We analyzed proliferation, functionality and morphogenesis during expansion and neural differentiation within these cultures. The use of FN-silk/LN-521 allows instant integration of hPSCs that can be expanded into shapeable, macro-sized 3D constructs for neuronal differentiation.

2. Materials and methods

2.1 Recombinant spider silk/laminin

The recombinant spider silk protein 4RepCT and functional variants thereof (VN-silk, FN-silk)[20,21,26] were supplied by Spiber Technologies AB (Sweden). Recombinant human laminin-521 was purchased from Biolamina (Sweden) and added to the silk protein solution at a final concentration of 10 μg ml^{-1}. The FN-silk/LN-521 mixture was incubated 5–10 min at RT before usage.

2.2 hPSC culture

hESC line HS980 with hPSCreg name Kle033-A, derived on LN-521,[24] was provided by Dr Hovatta, Karolinska University Hospital, Sweden. hiPS cell line C5, derived on fibroblasts and adapted to LN-521 as previously described,[21] was provided by Karolinska Institutet, Sweden, Falk lab. Both lines were used in agreements with ethical vetting by the Regional Ethics Board, Stockholm (Dnr 2015/824-39). The hPSCs were maintained at 37 °C, 5% CO_2 on LN-521 coated plates in Essential 8™ (ThermoFisher) with daily medium change. The cells were passaged with TrypLE (ThermoFisher) and counted manually before integration into silk scaffolds. Passages 11–25 were used in this study. Cell lines were routinely tested for mycoplasma 2–5 times a year.

2.3 Integration of hPSCs into silk foam and analysis of foam stability

Silk foam with integrated hPSCs were prepared in hydrophobic plates of 24-well format (Sarstedt cat no 83.3922.500). Porous foam was formed by rapidly pipetting air (2–3 strokes per s) using a pipette set at 40 μl into a droplet of 20 μl FN-silk/LN-521 placed at the bottom of a well and spread to a diameter of 1 cm. 50 000 hPSCs resuspended in culture medium (typically 10 000–15 000 cells per μl) in presence of 10 μg ml^{-1} Rock inhibitor Y27632 (VWR) were added directly into the foam and distributed by 5 additional strokes with the pipette. The foams were stabilized for 15 min at 37 °C, 5% CO_2 in a cell incubator before submerged with 0.7 ml Essential 8™ (ThermoFisher) supplemented with 10 μg ml^{-1} Y27632. Rock inhibitor was omitted in the medium from 16–20 hours after seeding. For evaluation of foam stability, 12 foams per condition were monitored by bright field microscopy 2 days after foam formation. Stability was graded as % of intact foam attached to the bottom of the well. After the air-bubbles have burst, the foam maintains at least 100 μm height, which, if assuming around 5 cell layers, a similar cell density as the 2D control (14×10^3 cells per cm^2).

2.4 Metabolic activity and proliferation

The metabolic activity, as a relative measurement of cell growth, was monitored by Alamar Blue cell viability assay (Invitrogen) at 48 h after cell-integration. Supernatants from cultures were measured after 2 h incubation with the Alamar blue reagent using a fluorescence plate reader (CLARIOstar, BMG Labtech). Fluorescence intensities from four cultures per condition were analyzed. For cell proliferation, 50 000 cells from HS980 and C5 were dissociated with TryLE and counted manually before seeding and at the endpoint (72 h). Proliferation is presented as fold change. For each experiment, cells from three different passages were analyzed.

2.5 Live/dead assay

Silk foams with integrated cells were washed once in pre-warmed PBS before 30 min incubation with calcein and EthD-1 (live/dead viability kit, Invitrogen). Imaging was performed on a Leica DMI6000 B. Images were processed using NIH Image J software.

2.6 Immunocytochemistry

Silk foams with integrated cells were washed once in PBS and fixed in 4% paraformaldehyde for 15 min at RT followed by three washes in PBS. For sectioning; fixed samples were incubated in 20% sucrose at 4 °C, over night before embedding in Tissue-Tek (Sakura) and sectioned using a Leica cryostat CM 1950. Permeabilization was done at RT for 15 min in PBS with 0.1% Triton X-100 followed by blocking for 1 h at RT with 10% donkey serum (Jackson ImmunoResearch). Primary antibodies were incubated overnight at 4 °C in PBS with 0.1% Tween-20 (PBST) and 5% donkey serum. Secondary antibodies were incubated for 1 h at RT in PBST with 5% serum. The samples were washed three times with PBST between each incubation. Primary antibodies: anti-OCT3/4 (R&D, #962649, 1 : 50), anti-NANOG (R&D, #963488, 1 : 50), anti-Laminin (Abcam, ab11575, 1 : 200), anti-PAX6 (Abcam, ab5790, 1 : 100), anti-Nestin (R&D, #196908, 1 : 200), anti-BIII-tubulin (Sigma, #SDL3D10, 1 : 500), anti-SOX2 (Santa Cruz, sc-17320, 1 : 50), anti-KI67 (Abcam, ab92742, 1 : 100), anti-N-cadherin (Abcam, ab12221, 1 : 200), anti-DCX (Abcam, ab18723, 1 : 200), anti-MAP2 (Sigma, #AP-20, 1 : 500), anti-GAD67 (Millipore, #1G102, 1 : 200). Secondary antibodies: anti-rabbit 647 (Abcam, ab150075, 1 : 1000), anti-goat 647 (Abcam, ab15031, 1 : 1000), anti-goat 488 (Jackson ImmunoResearch, 705545147, 1 : 1000), anti-mouse 488 (Jackson ImmunoResearch, 715545150, 1 : 1000). Nuclei were visualized with DAPI (Sigma). Slides were mounted in fluorescence mounting medium (DAKO). Fluorescence was analyzed on a Leica DMI6000 B, or for maximum intensity projection, a Zeiss Light Sheet Z.1 with 10×/0.5NA detection objective was used. Images were processed using NIH Image J software.

2.7 RNA isolation and gene expression analysis

Extraction of total RNA was carried out using a mini RNA purification kit (Qiagen). The RNA was reverse-transcribed using maxima first strand cDNA synthesis kit (ThermoFisher). Real-time qPCR was performed by TaqMan probe-based detection in a C1000™ Thermal Cycler (Bio-Rad) according to the manufacturer's instructions. TaqMan gene expression assays (Life Technologies) were used for: human *NANOG* ID Hs 04260366_g1, human *POU5F1* ID Hs 04260367_gH, human *B2M* ID 4333766, human *FOXG1* ID Hs 01850784_s1, human *TUB3* ID Hs 00801390_s1, human *PAX6* ID 00240871_m1, human *ZIC1* ID 00602749_m1, human *T* ID 00610080_m1. PrimePCR assays (Bio-Rad) *GAD1* Hsa, *MAP2* Hsa, *B2M* Hsa were analyzed with SsoAdvanced™ Universal SYBR® Green Supermix (Bio-Rad). *B2M* was used as an endogenous control and expression was quantified by $2^{-\Delta\Delta Ct}$.[27] Results from real time qPCR measurements were expressed as mean fold change ± standard deviation (n = 5) or as stated.

2.8 Quantification of cell growth

The cell expansion in foam was quantified using Hoechst-based DNA quantification (Sigma Aldrich). Foams with integrated HS980 cells were prepared as previously described and transferred to sterile nylon nets fitted in a 24-well culture plate to enable any cell debris to be easily removed from the culture. Whole foams with cells were harvested at indicated timepoints by freezing in PBE buffer (100 mM Na_2HPO, 5 mM Na_2EDTA at pH 7.5). Thawn samples were supplemented with 10 mM L-cysteine and 125 μg ml^{-1} papain enzyme (Sigma Aldrich) and digested at 60 °C over night. The DNA was quantified in a 96-well plate in 2 μg ml^{-1} Hoechst 33258 and 1× fluorescent assay buffer using a CLARIOstar microplate reader (BMG Labtech). Three samples per timepoint was plotted as average cell number ± standard deviation (n = 3).

2.9 Neural differentiation

Neural induction was initiated three days after integration into silk foam using a modified version of a dual-SMAD inhibition protoc.[28,29] The cells were cultured in neural induction medium (NIM) consisting of 50% Neurobasal medium (ThermoFisher) and 50% DMEM/F12 (ThermoFisher) supplemented with 0.5× B-27 without vitamin A (ThermoFisher), 0.5× N2 (ThermoFisher), 100 μM 2-mercaptoethanol (Sigma) and GlutaMAX (Life Technologies) with the addition of recombinant human Noggin, 500 ng ml^{-1} (R&D) and SB431542, 10 μM (Tocris) with daily medium change. After seven days, NIM was replaced by neuronal progenitor medium (NPDM); 50% neurobasal medium (ThermoFisher Scientific) and 50% DMEM/F12 (ThermoFisher) supplemented with 0.5× B-27 without vitamin A (ThermoFisher), 0.5× N2 (ThermoFisher), 100 μM 2-mercaptoethanol (Life Technologies) and GlutaMAX (Life Technologies). Medium was changed every second or third day for the remaining culture time.

2.10 Calcium imaging analysis

Calcium imaging using cell permeant Fluo-4, AM (Life Technologies) was performed according to manufacturer's protocol at day 40 and day 60. The silk foams with integrated cells were incubated in neural progenitor differentiation medium with Fluo-4 for 30 min. Images of fluorescence intensity over time were acquired with a Leica DMI6000 B at room temperature and analyzed using NIH Image J software. Calcium releases demonstrating spontaneous activity were visualized by spectra. Top view images using a ×10 objective of day 60 cultures, typically revealed up to 10% cells giving spontaneous calcium surges during a 3 min analysis period.

2.11 Statistical analysis

Data are presented as mean ± standard deviations. Statistical analyses were performed with Student t-test (preceded by One-way ANOVA when comparing multiple groups). Significant p values or non-significant values (n.s.) are reported for each

figure in the respective figure legend. For all tests a p-value <0.05 was considered statistically significant.

3. Results

3.1 A combination of FN-silk and laminin 521 support 3D culture of evenly integrated human pluripotent stem cells

Pre-made scaffolds of the recombinant spider silk proteins FN-silk and VN-silk has previously been found to promote cellular attachment and proliferation of cells seeded on top.[20,21] Here, we explored the possibility to integrate hPSCs into a 3D silk foam by allowing cells to be present during the silk-assembly, as described in Fig. 1A. A droplet of soluble silk protein is placed in the well of a hydrophobic culture plate. To transform the silk solution into a foam, air is repeatedly pipetted into the droplet at a speed of 2–3 strokes per s (i). Cells are prepared as a concentrated single-cell suspension in culture medium and added directly into the center of the foam (ii). To obtain a homogenous cell distribution, some additional strokes with the pipette are applied. The foam with integrated cells is then stabilized for 15 min in the cell incubator (iii) before addition of culture medium (iv. and Fig. 1B). Due to the pipetting, each air bubble within the foam is surrounded by a thin silk film. Within 1–3 days of culture, these films will burst, thereby transforming the foam into a network of microfibrillar silk with evenly integrated cells.[23]

In the early embryo, specific isoforms of laminin are expressed, including those with side chains α5β2γ1.[30] In

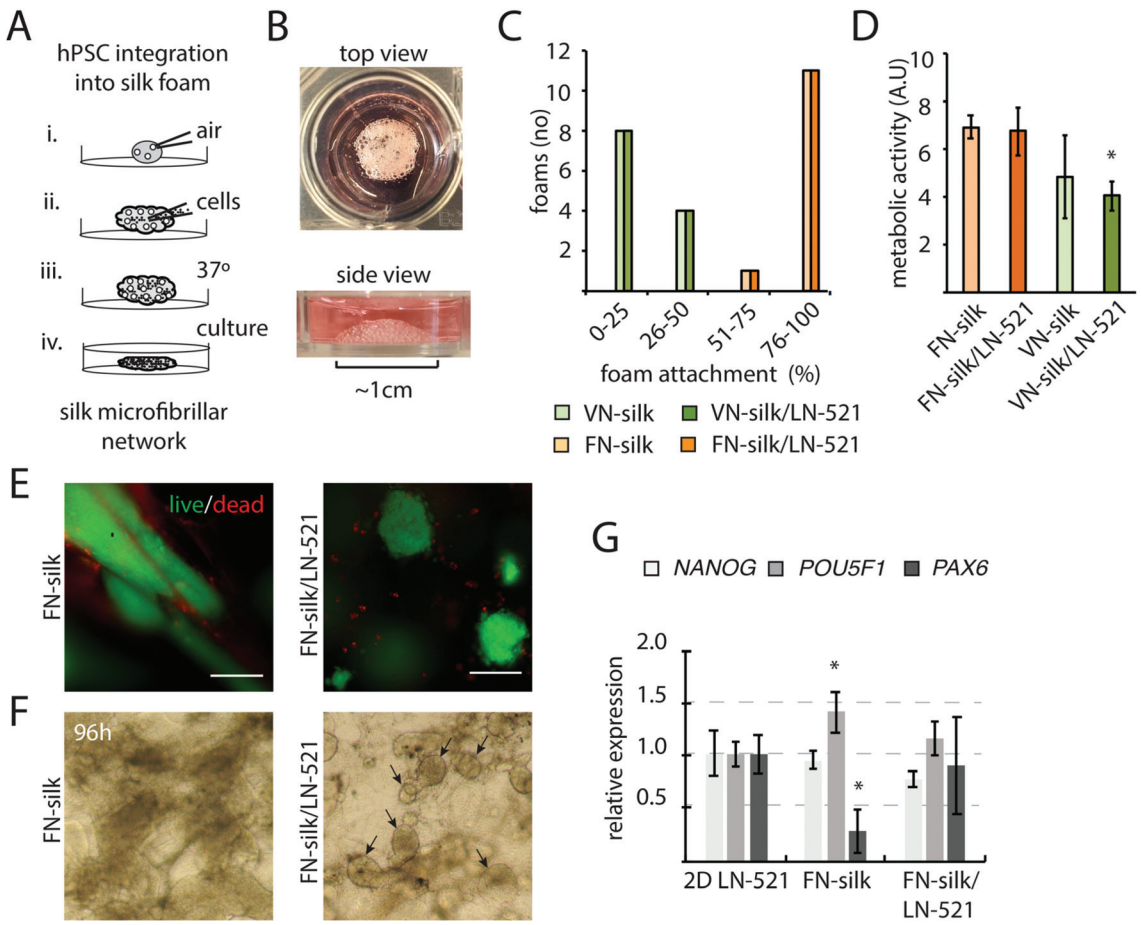

Fig. 1 Foam stability and cell expansion of integrated hPSCs in FN- and VN-silk with LN-521. (A) Schematic drawing of the procedure for integration of hPSCs into silk foam. A droplet (20 μl) of soluble FN silk protein (3 mg ml^{-1}) is placed on a hydrophobic surface. The solution is transformed into foam by rapidly pipetting air bubbles 20 times into the droplet (2–3 strokes per s) (i). A concentrated cell suspension (50 000 cells) is distributed in the foam by gentle pipetting(ii). The foam is stabilized at 37 °C for 15 min in the cell incubator (iii) before addition of culture medium (iv). (B) Top and side view of FN-silk/LN-521 foam with hPSCs after submerged in culture media. (C) Stability of VN- and FN-silk foams, with or without the addition of LN-521, two days after integration of cells. Bars represent percentage of foams still attached to the culture plate, as determined by microscopy analysis of 12 foams per condition. (D) Metabolic activity measured by AlamarBlue 48 h after integration. Data represent the mean ± SD (n = 4), * p < 0.05 as compared to FN-silk/LN521. (E) Cell viability and colony morphology 2 days after integration into FN-silk with or without the addition of LN-521. Viable cells were stained by calcein (green) and dead cells were visualized with EthD-1 (red). Scale bars = 100 μm. (F) Representative morphology of expanding colonies 4 days after integration into silk, as determined using a bright field microscope with ×10 objective. Black arrows indicate examples of regular shaped colonies. (G) Relative gene expression of HS980 at 4 days after integration into silk or cultures in 2D on LN521, analyzed by RT-qPCR for pluripotency markers *POU5F1* (white) *NANOG* (light grey) and *PAX6* (dark grey). Data show the mean fold change ± SD (n = 4), * p < 0.05 as compared to 2D control on LN-521.

culture, coatings of recombinant human LN-521 have been shown to promote survival, self-renewal and pluripotency.[24] To create a 3D niche suitable for hPSCs, a fraction of LN-521 was added to the silk solution before silk assembly. Cells of the human embryonic stem cell line, HS980, initially derived and cultivated on LN-521 [31] were then added. First, we investigated the stability of different variants of silk/laminin foams with integrated cells. FN-silk gave rise to stable foam structures, whereas the majority of the foams made of VN-silk were completely or partly disintegrated and detached from the bottom after a 48 h culture period (Fig. 1C). Addition of LN-521 showed no effect on foam stability nor on metabolic activity of the integrated cells (Fig. 1D), although the proliferation rate was lower in VN-silk/LN521, likely due to instability of the VN-silk itself. When comparing viability and colony morphology of cells seeded within FN-silk with and without LN-521, we noticed that cells formed dense and irregular aggregates without LN-521, while cells within FN-silk with LN-521 appeared in well-distributed and round colonies (Fig. 1E), which became more evident under the microscope after four days of culture (Fig. 1F). To further investigate cell behavior during expansion in FN-silk, gene expression analysis revealed slight variations of pluripotency marker *POU5f1* and the neural marker *PAX6* as compared to cells cultured on a tissue culture plate coated with LN-521 (Fig. 1G). However, the gene expression in cells cultured in FN-silk foam with LN-521 did not reveal this variation. Taken together, due to the irregular colony morphology and decrease of PAX6 in FN-silk without LN-521, we decided to continue further studies to promote neural differentiation in 3D using FN-silk with addition of LN-521.

3.2 Expanding hPSCs express pluripotency markers after integration into FN-silk/LN-521 foam

At initiation of a differentiation protocol, a homogenous starting cell population as well as proper cell densities are important factors,[32,33] and we therefore characterized the initial cell growth and pluripotency of cells seeded within the FN-silk/LN-521 foam. The introduction of air bubbles into the silk droplet enlarged its original size ~three times, resulting in a hemisphere-shaped foam with a diameter of 1 cm. One day after cell integration, the vast majority of the silk films surrounding the air-bubbles had burst, leaving evenly distributed cells attached to a network of silk/laminin microfibrils (Fig. 2A). After two days, the initially dispersed cells had formed small 3D colonies of $NANOG^+$ cells (Fig. 2B). The distance between the cell colonies were directly dependent on the volume of the silk solution and the number of cells integrated. When analyzing the cell proliferation for HS980 and a human induced pluripotent cell line (hiPS, C5)[21] after three days in FN-silk/LN-521 and compared with 2D control, no difference could be detected (Fig. 2D). At this stage, the majority of the cells had reached their logarithmic growth phase and the cell colonies covered the majority of the space within the microfibrillar network (ESI Fig. S1A†). Immunofluorescence analysis of the pluripotency markers NANOG and OCT4 revealed positive staining in all visible nuclei. The cell colonies had grown considerably in size compared to the time of cell integration (compare Fig. 1E, 2B with C). Gene expression analysis of the two cell lines cultured in FN-silk/LN-521 revealed similar levels of pluripotency markers (even slight increase for C5), when compared to cells grown in 2D on conventional tissue culture plates coated with LN-521 (Fig. 2E).

3.3 Induction of early neural progenitors in FN-silk/LN-521 foam

To test *in situ* differentiation towards neural linages in silk foam, we performed a series of trials using a general dual-SMAD inhibition protocol.[32] As previously described, pluripotent cells integrated into foams made of FN-silk/LN-521 can be expanded for 3 days to gain sufficient density for initiation of neural differentiation (Fig. 2). Neural differentiation was induced with a medium (NIM) including Noggin and SB431542 (Fig. 3A). After seven days, the colonies of neural progenitors had expanded throughout the foam (Fig. 3B). Immunofluorescence analysis of cells integrated in the foam revealed a homogenous distribution of $PAX6^+$ and symmetrically distributed N-CAD staining, at this stage similar to cells grown as monolayer on LN-521 coatings (Fig. 3C).

Temporal gene expression analysis confirmed rapid induction of early neural markers *PAX6*, *ZIC1* and *FOXG1* in cells integrated in foam (Fig. 3D). Notably, in early induction up to day 5, the expression of the three neural markers were found equal to or slightly higher for cells integrated in FN-silk/LN-521 foam than in controls on LN-521 coatings. This was mirrored by a somewhat quicker drop in pluripotency marker *POU5f1.* At day 7, no major differences in loss of pluripotency marker *POU5f1* or T-box transcription factor, a marker for epithelial-to-mesenchymal transition, were detected. Taken together, the abundancy of early neural markers and a rapid loss of pluripotency indicated that the combination of FN-silk/LN-521 would be a suitable platform for neural differentiation in a 3D culture.

3.4 Formation of continuous neuroectodermal 3D structures in FN-silk/LN-521 foam

With the aim to form controlled, homogenous 3D populations of neural progenitors for further neuronal differentiation, we assessed the first steps of neurogenesis in defined x, y, z axis planes of foams. Cell integration, expansion and neural induction was initiated as described above (including 7 days in NIM medium), before switching to a neural progenitor medium without the inhibitors (ESI Fig. S2A†). Foams with integrated cells were fixed at day 14 and sectioned as indicated in Fig. 4A. The foams, 1 cm in diameter, contained cells arranged in layers with a total approximate height of 100–150 μm (Fig. 4B). At this stage, we observed a homogenous cell distribution throughout the entire section with strongly expressed early neural markers PAX6 and NESTIN, neural stem cell marker SOX2 and the proliferation marker KI67 (Fig. 4B), indicating dividing progenitors throughout the vertical plane. From analyses of multiple horizontal sections, we noticed that the pores

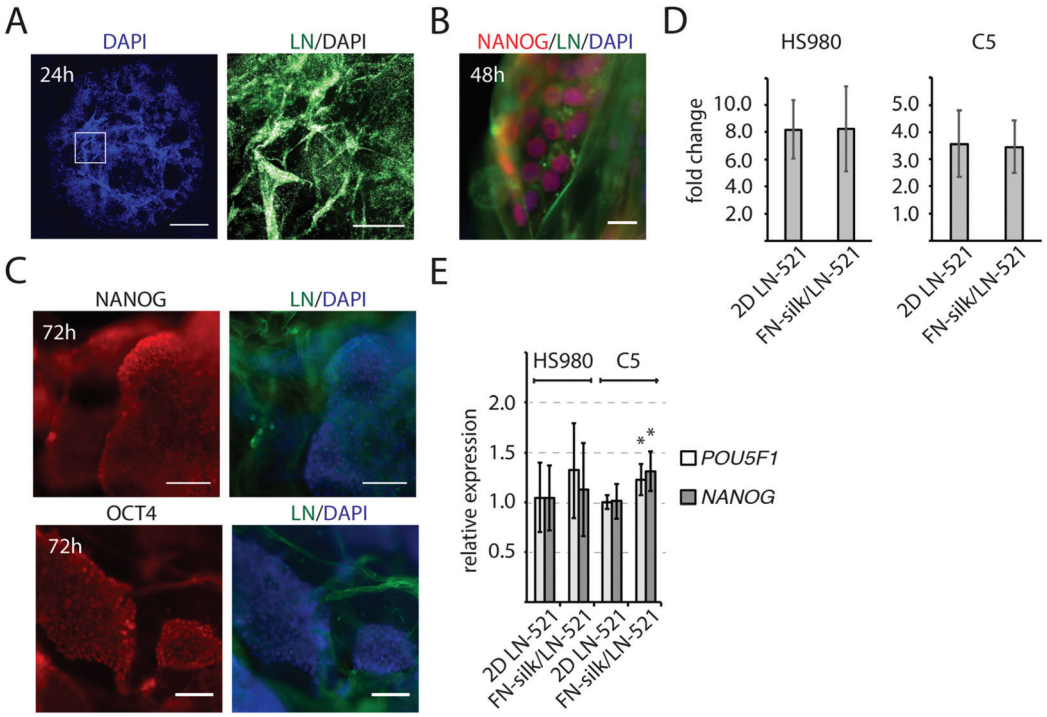

Fig. 2 Cell distribution and pluripotency of hPSCs after integration to FN-silk/LN-521 foam. (A) Stitched micrograph of the entire FN-silk/LN-521 foam 24 h after seeding cells (DAPI stained nuclei in blue)(left image). Scale bar = 2 mm. White box indicate magnified area (right image). Microfibrillar structure of the FN-silk/LN-521 foam, visualized by immunofluorescence analysis of laminin (LN, green). Nuclei of integrated cells are stained by DAPI (white). Scale bar = 100 μm. (B) Typical morphology of a hPSC colony 48 h after integration into silk (laminin, LN, green). Immunofluorescence analysis of pluripotency marker NANOG in red and DAPI in blue. Scale bar = 20 μm. (C) Immunofluorescence analysis of pluripotency markers NANOG (upper panels) and OCT4 (lower panels) in red, at 72 h. Cell nuclei and FN-silk/LN-521 were visualized by DAPI (blue) and laminin (LN, green), respectively. Scale bars = 100 μm. (D) Cell expansion for HS980 and C5 in FN-silk/LN-521 foam compared to tissue culture pate coated with LN-521 at 72 h after seeding. Data show the mean fold change ± SD from three different passages. (E) Relative gene expression of *POU5F1* (white) and *NANOG* (dark grey) for HS980 and C5 at 72 h after integration to FN-silk/LN-521 as compared to culture on tissue culture plates with LN-521 coatings. Data show the mean fold change ± SD (n = 5).

of the fibrillar silk network had developed into channels throughout the 3D culture (Fig. 4C, white asterisks). These channels facilitate access of media for also the innermost cells inside the silk network. Cells co-expressing PAX6 and SOX2, as well as uniformly distributed KI67$^+$ cells, were found throughout the cultures in all horizontal and vertical sections analyzed (Fig. 4B and C). Furthermore, cells positive for neural marker NESTIN were prominent, as well as cells displaying the neuronal marker BIII-TUBULIN, confirming differentiation into neuroectoderm (Fig. 4C and D). Gene expression analysis showed induction of *PAX6* and *FOXG1*, while the pluripotency marker *POU5f1* was markedly reduced (ESI Fig. S2B†). At day 17, also DCX, a marker of newborn neurons, was clearly visible along with the PAX6$^+$ cells (Fig. 4E). Together, these results show an effective and uniform differentiation of hPSCs towards a neuroepithelial fate in the centimeter-sized FN-silk/LN-521 network.

3.5 Generation of neuronal progenitors in FN-silk/LN-521 foam

To evaluate the potential of FN-silk/LN-521 silk to support development of neurons, we extended the cultivation period in neuronal progenitor medium for a general differentiation without additional patterning factors. The appearance of neuronal markers was analyzed after 3 and 6 weeks. An intricate 3D network of a mixture of cells positive for BIII-TUBULIN and for MAP2 (more mature neurons), was observed at day 21 (Fig. 5A) which was further developed one week later (Fig. 5D). In addition, GADD67$^+$ cells were found integrated within the silk microfibrils, indicative of development of inhibitory GABAergic interneurons. Transcription analysis showed strong expression of BIII-TUBULIN and MAP2 (Fig. 5B). Up-regulation of GAD1, an additional marker for GABAergic interneurons, confirmed the presence of cells of interneuronal subtypes.

In contrast to the uniform distribution of cells expressing markers for cycling progenitors found at day 14 (see Fig. 4B and C), analysis of horizontal sections at day 21 showed a more heterogeneous pattern of KI67$^+$ cells, preferentially residing at the walls of the channels (Fig. 5C). This was further visualized by the abundance of neural stem cell marker SOX2, indicating that many of the progenitors within the 3D culture remained in their early state of differentiation.

After a culture period extended to 40 days, analysis of vertical sections revealed MAP2$^+$ cells throughout the foam struc-

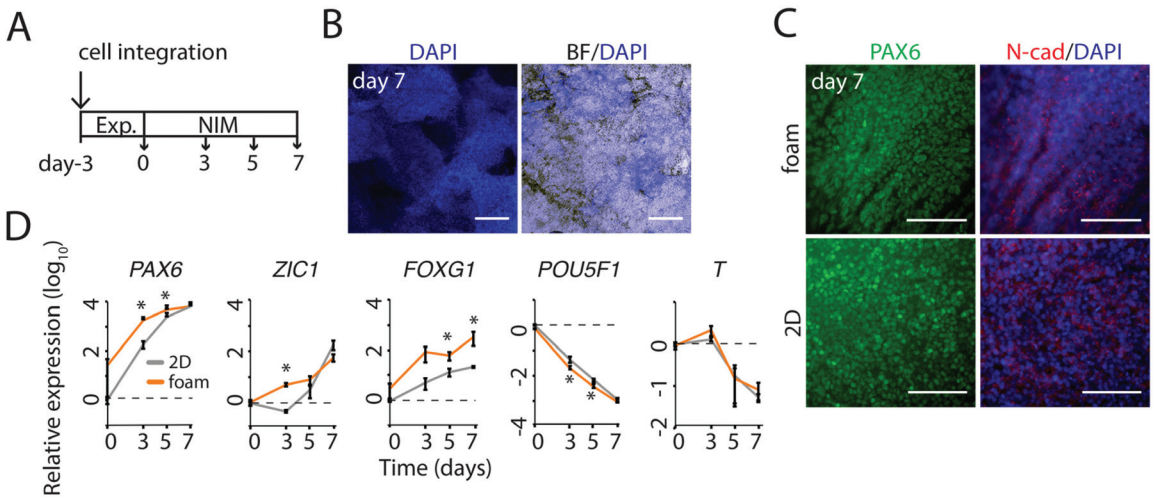

Fig. 3 Early neural induction in silk foam. (A) Schematic illustration of the protocol used. After cell integration into silk foam (large arrow), hPSCs were expanded (Exp.) in pluripotency medium for 72 h, followed by culture in neural induction medium (NIM). Cell samples were harvested for analysis at indicated time points (small arrows). (B) Representative colony organization within the silk at day 7, shown by DAPI stain (blue, left) and overlay with bright field to visualize the silk microfibrils (grey, right). Scale bars = 200 μm. (C) Morphology of cells with neuroectodermal marker PAX6 (green) and neuroepithelial marker N-cad (red) in foam, as compared with 2D culture. Scale bars = 100 μm. (D) Time-dependent gene expression in foam compared to 2D cultures, analyzed at day 0, 3, 5 and 7. Data show induction of neural markers (*PAX6*, *ZIC1*, *FOXG1*) and down regulation of pluripotency marker (*POU5f1*), and mesodermal marker (*T*). Bars represent the mean fold change ± SD (n = 4), * $p < 0.05$ as compared to 2D control on LN-521.

ture, but especially on the upper side (Fig. 5E). At this stage, the total construct of cells within silk had typically grown to a height of >200 μm. Horizontal sections revealed loose structures of cells at different stages of neurogenesis. No necrotic areas were found, even when analyzing the inner parts. Partial expression of neural stem cell markers SOX2 and PAX6 remained within the 3D culture, preferentially in areas of lower cell density (ESI Fig. S3A†), or next to the channels (Fig. 5F). When analyzing sequential sections, KI67 staining confirmed the presence of cycling cells, flanked by more mature neurons ($MAP2^+$) (Fig. 5F and G). To summarize, generation of hPSC-derived neuronal progenitors integrated in the FN-silk/LN-521 microfibrillar network is a simple way to efficiently obtain a continuous 3D distribution of the cell types that constitute the foundation of the developing brain.

3.6 Neural progenitors retain self-organizing ability in FN-silk/LN-521

Pluripotent stem cells and early progenitors have a strong self-organizing ability to regulate the development, which can be utilized to obtain organ-like units *in vitro*.[34] After longer cultivations in FN-silk/LN-521, zones of cycling progenitor cells were found organized into polarized cellular organizations (ESI Fig. S3†). These findings encouraged us to further investigate whether FN-silk/LN-521 3D cultures would provide a suitable microenvironment for supporting self-organization during differentiation.

We reasoned that cellular self-organization would be facilitated by increasing the flexibility of the silk construct. To test this, we first used the protocol described above to generate homogeneous layers of neuronal progenitors in FN-silk/LN-521. The silk foams with integrated progenitors were then manually detached from the bottom of the wells, cut into slices of ≈2 mm thickness and transferred to low-attachment culture plates where they were kept as floating entities (Fig. 6A). By further extending the cultivation time, this allowed the cells to spontaneously reorganize within the silk network and the cellular constructs to grow in size.

Immunofluorescence analysis of 3D cultures sectioned 60 days after initiation of differentiation revealed multiple regions of $SOX2^+$ cell populations radially organized around the channels and surrounded by layers of cells positive for BIII-TUBULIN (Fig. 6B). The internal structures are an indicative of neural stem cell organization and highly reminiscent of the ventricular zones formed during early neural tube development, which has previously been modeled in cerebral organoids.[4] Looking more closely within the 3D culture, multiple columnar shaped organizations of $SOX2^+$ and $NESTIN^+$ cells surrounding ventricle-like cavities with apical localization of the neural specific N-cadherin were found (Fig. 6C). Many of these regions also contained layers of $PAX6^+$ cells, surrounded by newborn neurons marked by DCX^+ cells at the basal surface.

3.7 FN-silk/LN-521 supports the generation of cells displaying spontaneous calcium oscillations

To test whether the progenitors that had formed within the FN-silk/LN-521 cultures were functionally active, we imaged the cells after treatment with the calcium indicator Fluo-4. At day 40, widespread spikes in intracellular calcium concen-

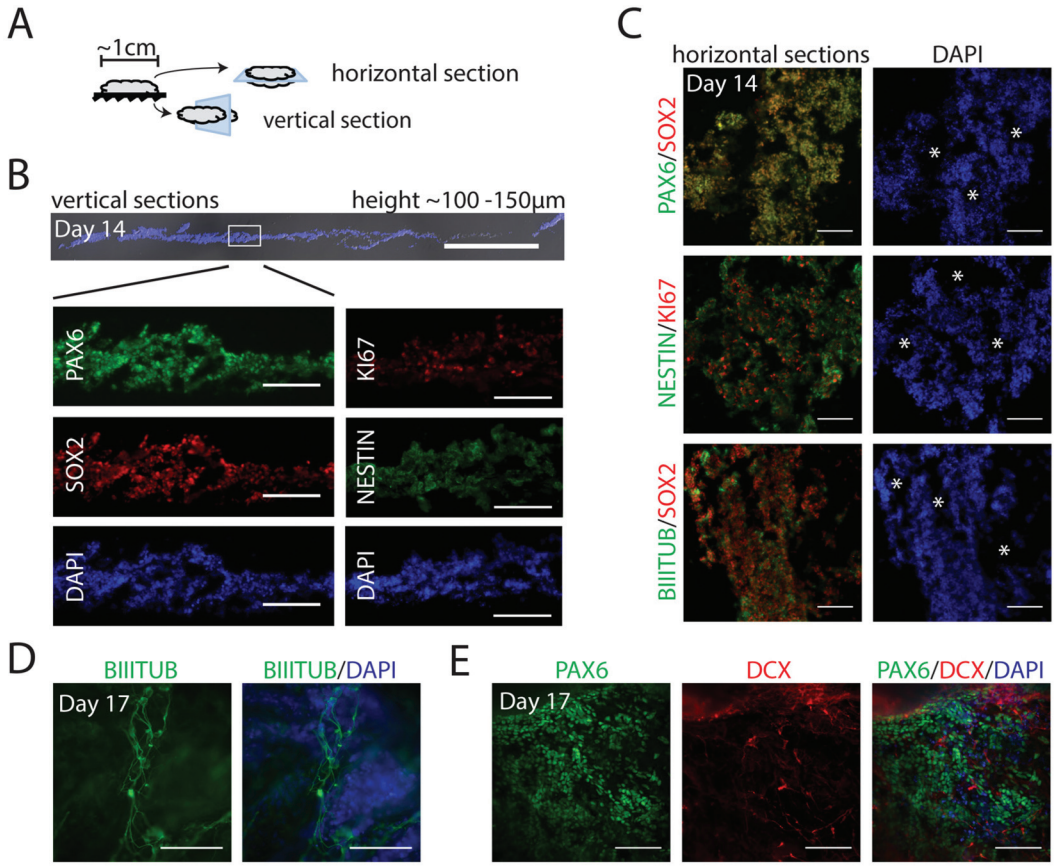

Fig. 4 Homogenous neuroectoderm formation in FN-silk/LN-521 foam. (A) Illustration describing vertical and horizontal sectioning of FN-silk/LN-521 foams with integrated cells. (B) Immunofluorescence analysis of part of a vertical section (bright field (grey) overlaid with DAPI in blue) including magnified areas (below) analyzed for neural progenitor marker PAX6, neural marker NESTIN and neural proliferation marker SOX2 and proliferation marker KI67. Scale bars = 1 mm for the overlaid section and 200 µm for the magnified vertical sections. (C) Horizontal sections show co-expression of PAX6 (green) and SOX2 (red) (upper). White asterisks mark spontaneously formed channels within the silk network filled with culture medium. Evenly distributed NESTIN (green) and KI67 (red) and BIII-TUBULIN (green) and SOX2 (red). Nuclei are counterstained with DAPI (blue). (D) Side-view of foam stained for BIII-TUBULIN (green) and analyzed by light sheet microscopy at day 17 and (E) DCX (red) and PAX6 (green) and DAPI (blue). Scale bars = 100 µm for (C), (D) and (E).

tration [Ca^{2+}] were seen, indicating spontaneous activity (ESI Fig. S3B†). In addition, areas of sequential activity involving several cells were observed. Similar spontaneous calcium activity was also noticed at day 60 (Fig. 6D, n = 3), and ESI Movie 1.† Together, this demonstrates the ability of hPSC-derived neural progenitors to spontaneously form cerebral structures with active, signaling progenitors, thereby recapitulating the early neurodevelopment.

4. Discussion

In this study we developed a fully defined 3D culture setup for neural differentiation of human pluripotent stem cells using a functionalized recombinant silk protein, FN-silk[20] in combination with recombinant laminin, LN-521.[24] The procedure to instantly integrate pluripotent stem cells during silk assembly resulted in centimeter-sized 3D constructs, suitable for differentiation and long-term cell survival. We found that this culture set-up provides an easy method for engineering of constructs such as layers of continuous neuroectoderm, network with neuronal activity and self-organizing neural tube-like structures. The method described here constitutes a viable base also for the development of a variety of neuronal differentiation protocols for hPSCs in 3D formats.

Cell density is an important factor for neural differentiation outcome[32] and at the same time a challenge for any 3D culture set up. The procedure for integration of cells into FN-silk/LN-521 foam involves a mild dispersion of single cells before stabilization, resulting in an even distribution of cells within a network of flexible silk microfibers and laminin. By adjusting the number of hPSCs at integration and the time of cell expansion, different densities of integrated cells are easily obtained. Herein, we used 50 000 pluripotent cells during seeding, rendering ~14 × 10^3 cells per cm^2 silk foam if assuming 4–5 cell layers. The fact that the hPSCs survive the integration process and stay pluripotent indicates that the silk/laminin is able to provide supportive cell-matrix contact points. After an initial

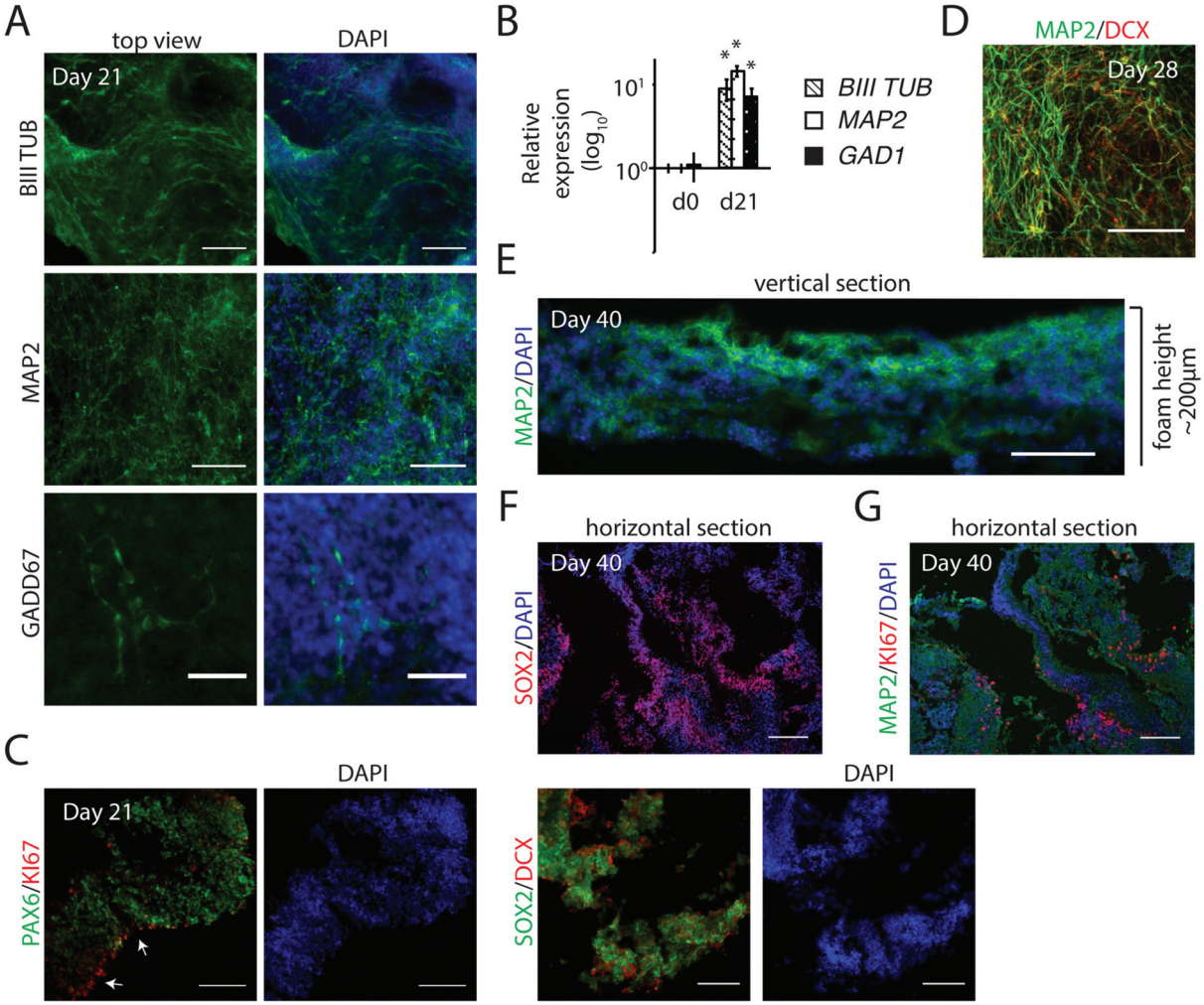

Fig. 5 Generation of neuronal progenitors by integration in FN-silk/LN-521. (A) Immunofluorescence analysis of neuronal marker BIII-TUBULIN, post-mitotic neuronal marker MAP2 and specific neuronal marker GADD67 at day 21. Nuclei are stained with DAPI in blue. Scale bars = 100 µm for stains with BIII-TUBULIN and MAP2, and 50 µm for GADD67. (B) Relative gene expression analyzed by RT-qPCR of neuronal markers at day 0 and day 21. All data represent the mean ± SD (n = 5), * $p < 0.05$ compared to day 0 before induction. (C) Immunofluorescence analysis of PAX6 (green) and KI67 (red, indicated by white arrows), and SOX2 (green) and DCX (red) in horizontal sections at day 21. DAPI in blue. Scale bars = 100 µm. (D) Immunofluorescence analysis of MAP2 (green) and DCX (red) by Light sheet microscopy at day 28. Scale bar = 100 µm. (E) Immunofluorescence analysis of vertical section visualizing MAP2 (green) and DAPI (blue) at day 40. The height of the foams with integrated cells had grown to around 200 µm. Scale bar = 100 µm. (F) and (G) Immunofluorescence analysis of sequential horizontal sections of the inner part at day 40, depicturing cells expressing SOX2 (red) in (E) and KI67 (red) surrounded by $MAP2^+$ cells (green) in (G). DAPI in blue. Scale bars = 200 µm.

culture period in neural induction medium, a defined and homogenous neural population forms a uniform layer of $SOX2^+$ and $PAX6^+$ neuroectoderm (Fig. 4). Advantages of using a biomaterial-based approach for engineering 3D constructs are the higher degree of control of the microenvironment and the possibility to obtain scalable constructs.[8] With this silk-based culture system it would be feasible to create combinations and/or gradients of *e.g.* different laminin isoforms or other extra cellular matrix proteins for the study of cell fate in 3D.

Many applications for neural modelling using hPSCs involve long-term differentiation protocols to obtain functionality of a specific cell type, such as oligodendrocytes,[35] or the maturation of higher order self-organizing brain structures, as for example formation of the cortical plate.[12] Herein, we show that during culture of cells supported by silk, channels are formed within the network of silk microfibers. These channels facilitate access of oxygen and nutrients throughout the construct which enable long term (>month-long) differentiations to be performed also without applying a flow. Analyses of sections from the inner part of the constructs confirmed that cells maintain viable and dividing progenitor cells were found also after a longer culture period, indicating sufficient permeability throughout the construct (Fig. 5F and G).

Pluripotent stem cells and early progenitors have a strong ability to self-organize into layered structures of cortical tissue,

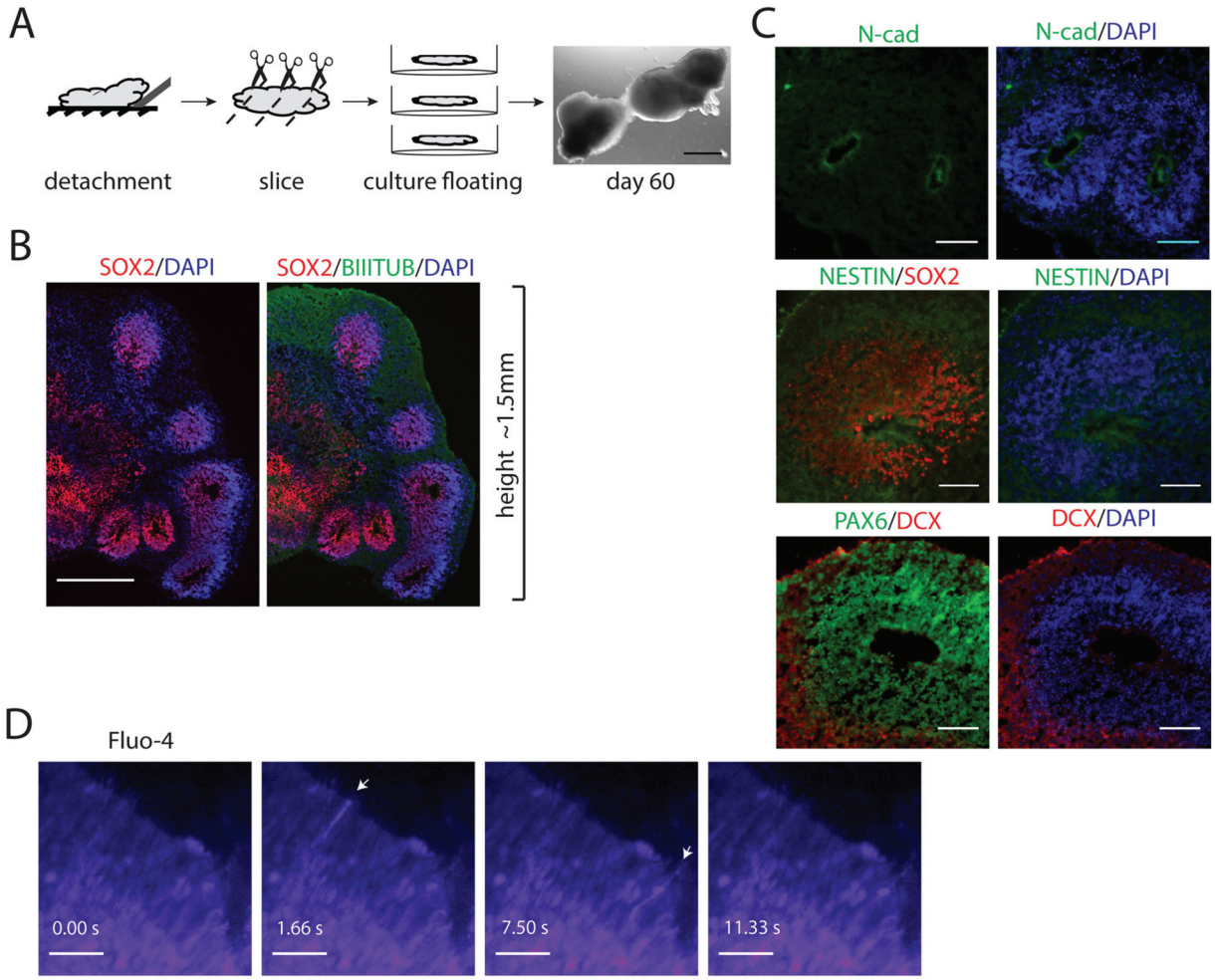

Fig. 6 Self-organized neural tube-like structures and neuron functionality in floating FN-silk/LN-521 constructs. (A) Schematic illustration of the procedure used for detaching silk foams for increased flexibility to allow cellular self-organization. After neuroectoderm formation, the foams with integrated neuronal progenitors were detached from the bottom of the well and transferred to low-attachment plates. The cell construct was cut into ≈2 mm thick slices and further cultured floating. Right: Representative image of a floating cell construct at day 60. (B) Section of a floating cell construct stained for SOX2 (red) and DAPI (blue) revealed proliferative zones developing around multiple ventricular-like regions, surrounded by BIII-TUBULIN (green) at the basal surface. (C) Immunostaining for N-cad (green) visualizing the apical surface of radially arranged cells (upper). NESTIN (green) and SOX2 (red) demonstrating the presence of neural progenitor zones (middle) and $PAX6^+$ cells (green) surrounded by layers of DCX^+ cells (red, bottom). Scale bars = 100 μm. (D) Live calcium imaging (Fluo-4) of FN-silk/LN-521 foam constructs at day 60, demonstrating spontaneous activity in progenitors developed during self-organization. Calcium releases were visualized by spectra (imageJ). Arrowheads points at active cells. Time in seconds is shown below. Scale bar = 40 μm.

closely resembling the human fetal brain.[36] Establishing robust protocols for such complex 3D cultures with reduced variations and using defined materials is important to be able to efficiently model the neural development and disease.[37] The silk/laminin microfibrillar network was found to be highly flexible and able to support extensive cellular remodeling during differentiation. Increasing the flexibility further by detaching the cell-silk construct from its support enhanced spontaneous reorganization into polarized neuroectoderm, allowing development of neural-tube like structures (Fig. 6). By this, we showed that the key steps during early neural development can be recapitulated in FN-silk/LN-521 matrix in similar ways as in spheroid-based cerebral organoids.[4,5]

The ability to create oriented and multi-layered cultures is attractive for mimicking the complex *in vivo* situation of tissue.[38] Combining several foams with integrated cells next to or on top of each other would be a feasible approach for the study of interactions between brain regions, similar to what has been demonstrated using fused cerebral organoids.[39] We recently described the possibility to integrate multiple cell types in FN-silk, including endothelial cells for *in vitro* vascularization.[23] Previously, this type of recombinant spider silk was shown to be degraded within 3 months after transplantation.[40] The 3D culture approach described herein could thus potentially be used for *in vivo* applications.

5. Conclusions

By assembly of recombinant functionalized silk protein together with laminin 521, we created a defined 3D silk fibrillar network for expansion and long-term differentiation of hPSCs. The mild assembly process of the silk enables an even integration of viable cells, creating a controlled and homogeneous neural population rendering functionally active neurons. Transfer of these flexible constructs into free-floating entities allowed development of neural tube like-tissue including progenitor polarity. Our results suggest that FN-silk/LN521 assembly could be a useful tool for a wide range of 3D culture aiming for neural tissue engineering.

Conflicts of interest

M.H. has shares in Spiber Technologies AB, a company that aims to commercialize recombinant spider silk.

Acknowledgements

We thank Spiber Technologies AB for providing recombinant spider silk proteins. We are grateful to Dr Steven Edwards at Advanced Light Microscopy Facility at SciLifeLab, Solna and the National Microscopy Infrastructure, NMI (VR-RFI 2016-00968) for providing assistance in microscopy and to the iPS Core at Karolinska Institutet, Stockholm.

References

1 K. A. Lemke, A. Aghayee and R. S. Ashton, Deriving, regenerating, and engineering CNS tissues using human pluripotent stem cells, *Curr. Opin. Biotechnol.*, 2017, **47**, 36–42.
2 M. Eiraku, K. Watanabe, M. Matsuo-Takasaki, M. Kawada, S. Yonemura, M. Matsumura, T. Wataya, A. Nishiyama, K. Muguruma and Y. Sasai, Self-organized formation of polarized cortical tissues from ESCs and its active manipulation by extrinsic signals, *Cell Stem Cell*, 2008, **3**(5), 519–532.
3 T. Nakano, S. Ando, N. Takata, M. Kawada, K. Muguruma, K. Sekiguchi, K. Saito, S. Yonemura, M. Eiraku and Y. Sasai, Self-Formation of Optic Cups and Storable Stratified Neural Retina from Human ESCs, *Cell Stem Cell*, 2012, **10**(6), 771–785.
4 M. A. Lancaster, M. Renner, C.-A. Martin, D. Wenzel, L. S. Bicknell, M. E. Hurles, T. Homfray, J. M. Penninger, A. P. Jackson and J. A. Knoblich, Cerebral organoids model human brain development and microcephaly, *Nature*, 2013, **501**, 373.
5 X. Qian, Ha N. Nguyen, M. M. Song, C. Hadiono, S. C. Ogden, C. Hammack, B. Yao, G. R. Hamersky, F. Jacob, C. Zhong, K.-j. Yoon, W. Jeang, L. Lin, Y. Li, J. Thakor, D. A. Berg, C. Zhang, E. Kang, M. Chickering, D. Nauen, C.-Y. Ho, Z. Wen, K. M. Christian, P.-Y. Shi, B. J. Maher, H. Wu, P. Jin, H. Tang, H. Song and G.-l. Ming, Brain-Region-Specific Organoids Using Mini-bioreactors for Modeling ZIKV Exposure, *Cell*, 2016, **165**(5), 1238–1254.
6 J. Mariani, G. Coppola, P. Zhang, A. Abyzov, L. Provini, L. Tomasini, M. Amenduni, A. Szekely, D. Palejev, M. Wilson, M. Gerstein, E. L. Grigorenko, K. Chawarska, K. A. Pelphrey, J. R. Howe and F. M. Vaccarino, FOXG1-Dependent Dysregulation of GABA/Glutamate Neuron Differentiation in Autism Spectrum Disorders, *Cell*, 2015, **162**(2), 375–390.
7 A. M. Paşca, S. A. Sloan, L. E. Clarke, Y. Tian, C. D. Makinson, N. Huber, C. H. Kim, J.-Y. Park, N. A. O'Rourke, K. D. Nguyen, S. J. Smith, J. R. Huguenard, D. H. Geschwind, B. A. Barres and S. P. Paşca, Functional cortical neurons and astrocytes from human pluripotent stem cells in 3D culture, *Nat. Methods*, 2015, **12**, 671.
8 S. B. Shah and A. Singh, Cellular self-assembly and biomaterials-based organoid models of development and diseases, *Acta Biomater.*, 2017, **53**, 29–45.
9 S. Knowlton, Y. Cho, X.-J. Li, A. Khademhosseini and S. Tasoglu, Utilizing stem cells for three-dimensional neural tissue engineering, *Biomater. Sci.*, 2016, **4**(5), 768–784.
10 R. Peerani, B. M. Rao, C. Bauwens, T. Yin, G. A. Wood, A. Nagy, E. Kumacheva and P. W. Zandstra, Niche-mediated control of human embryonic stem cell self-renewal and differentiation, *EMBO J.*, 2007, **26**(22), 4744.
11 Y. Li, M. Liu, Y. Yan and S.-T. Yang, Neural differentiation from pluripotent stem cells: The role of natural and synthetic extracellular matrix, *World J. Stem Cells*, 2014, **6**(1), 11–23.
12 M. A. Lancaster, N. S. Corsini, S. Wolfinger, E. H. Gustafson, A. W. Phillips, T. R. Burkard, T. Otani, F. J. Livesey and J. A. Knoblich, Guided self-organization and cortical plate formation in human brain organoids, *Nat. Biotechnol.*, 2017, **35**, 659.
13 B. J. Klotz, L. A. Oosterhoff, L. Utomo, K. S. Lim, Q. Vallmajo-Martin, H. Clevers, T. B. F. Woodfield, A. Rosenberg, J. Malda, M. Ehrbar, B. Spee and D. Gawlitta, A Versatile Biosynthetic Hydrogel Platform for Engineering of Tissue Analogues, *Adv. Healthcare Mater.*, 2019, **8**(19), e1900979.
14 K. Saha, A. J. Keung, E. F. Irwin, Y. Li, L. Little, D. V. Schaffer and K. E. Healy, Substrate Modulus Directs Neural Stem Cell Behavior, *Biophys. J.*, 2008, **95**(9), 4426–4438.
15 A. Ranga, M. Girgin, A. Meinhardt, D. Eberle, M. Caiazzo, E. M. Tanaka and M. P. Lutolf, Neural tube morphogenesis in synthetic 3D microenvironments, *Proc. Natl. Acad. Sci. U. S. A.*, 2016, **113**(44), E6831.
16 C. Allmeling, A. Jokuszies, K. Reimers, S. Kall, C. Y. Choi, G. Brandes, C. Kasper, T. Scheper, M. Guggenheim and P. M. Vogt, Spider silk fibres in artificial nerve constructs promote peripheral nerve regeneration, *Cell Proliferation*, 2008, **41**(3), 408–420.

17 C. Radtke, C. Allmeling, K. H. Waldmann, K. Reimers, K. Thies, H. C. Schenk, A. Hillmer, M. Guggenheim, G. Brandes and P. M. Vogt, Spider silk constructs enhance axonal regeneration and remyelination in long nerve defects in sheep, *PLoS One*, 2011, **6**(2), e16990.

18 M. Lewicka, O. Hermanson and A. U. Rising, Recombinant spider silk matrices for neural stem cell cultures, *Biomaterials*, 2012, **33**(31), 7712–7717.

19 M. D. Tang-Schomer, J. D. White, L. W. Tien, L. I. Schmitt, T. M. Valentin, D. J. Graziano, A. M. Hopkins, F. G. Omenetto, P. G. Haydon and D. L. Kaplan, Bioengineered functional brain-like cortical tissue, *Proc. Natl. Acad. Sci. U. S. A.*, 2014, **111**(38), 13811–13816.

20 M. Widhe, N. D. Shalaly and M. Hedhammar, A fibronectin mimetic motif improves integrin mediated cell biding to recombinant spider silk matrices, *Biomaterials*, 2016, **74**, 256–266.

21 S. Wu, J. Johansson, P. Damdimopoulou, M. Shahsavani, A. Falk, O. Hovatta and A. Rising, Spider silk for xeno-free long-term self-renewal and differentiation of human pluripotent stem cells, *Biomaterials*, 2014, **35**(30), 8496–8502.

22 S. Wu, J. Johansson, O. Hovatta and A. Rising, Efficient passage of human pluripotent stem cells on spider silk matrices under xeno-free conditions, *Cell. Mol. Life Sci.*, 2016, **73**(7), 1479–1488.

23 U. Johansson, M. Widhe, N. D. Shalaly, I. L. Arregui, L. Nilebäck, C. P. Tasiopoulos, C. Åstrand, P.-O. Berggren, C. Gasser and M. Hedhammar, Assembly of functionalized silk together with cells to obtain proliferative 3D cultures integrated in a network of ECM-like microfibers, *Sci. Rep.*, 2019, **9**(1), 6291.

24 S. Rodin, L. Antonsson, C. Niaudet, O. E. Simonson, E. Salmela, E. M. Hansson, A. Domogatskaya, Z. Xiao, P. Damdimopoulou, M. Sheikhi, J. Inzunza, A.-S. Nilsson, D. Baker, R. Kuiper, Y. Sun, E. Blennow, M. Nordenskjöld, K.-H. Grinnemo, J. Kere, C. Betsholtz, O. Hovatta and K. Tryggvason, Clonal culturing of human embryonic stem cells on laminin-521/E-cadherin matrix in defined and xeno-free environment, *Nat. Commun.*, 2014, **5**, 3195.

25 N. Polisetti, L. Sorokin, N. Okumura, N. Koizumi, S. Kinoshita, F. E. Kruse and U. Schlotzer-Schrehardt, Laminin-511 and -521-based matrices for efficient ex vivo-expansion of human limbal epithelial progenitor cells, *Sci. Rep.*, 2017, **7**(1), 5152.

26 M. Widhe, U. Johansson, C.-O. Hillerdahl and M. Hedhammar, Recombinant spider silk with cell binding motifs for specific adherence of cells, *Biomaterials*, 2013, **34**(33), 8223–8234.

27 K. J. Livak and T. D. Schmittgen, Analysis of Relative Gene Expression Data Using Real-Time Quantitative PCR and the 2−ΔΔCT Method, *Methods*, 2001, **25**(4), 402–408.

28 S. M. Chambers, C. A. Fasano, E. P. Papapetrou, M. Tomishima, M. Sadelain and L. Studer, Highly efficient neural conversion of human ES and iPS cells by dual inhibition of SMAD signaling, *Nat. Biotechnol.*, 2009, **27**(3), 275–280.

29 C. Nicoleau, C. Varela, C. Bonnefond, Y. Maury, A. Bugi, L. Aubry, P. Viegas, F. Bourgois-Rocha, M. Peschanski and A. L. Perrier, Embryonic stem cells neural differentiation qualifies the role of Wnt/beta-Catenin signals in human telencephalic specification and regionalization, *Stem Cells*, 2013, **31**(9), 1763–1774.

30 E. Klaffky, R. Williams, C.-C. Yao, B. Ziober, R. Kramer and A. Sutherland, Trophoblast-Specific Expression and Function of the Integrin α7 Subunit in the Peri-implantation Mouse Embryo, *Dev. Biol.*, 2001, **239**(1), 161–175.

31 S. Rodin, L. Antonsson, C. Niaudet, O. E. Simonson, E. Salmela, E. M. Hansson, A. Domogatskaya, Z. Xiao, P. Damdimopoulou, M. Sheikhi, J. Inzunza, A. S. Nilsson, D. Baker, R. Kuiper, Y. Sun, E. Blennow, M. Nordenskjold, K. H. Grinnemo, J. Kere, C. Betsholtz, O. Hovatta and K. Tryggvason, Clonal culturing of human embryonic stem cells on laminin-521/E-cadherin matrix in defined and xeno-free environment, *Nat. Commun.*, 2014, **5**, 3195.

32 S. M. Chambers, C. A. Fasano, E. P. Papapetrou, M. Tomishima, M. Sadelain and L. Studer, Highly efficient neural conversion of human ES and iPS cells by dual inhibition of SMAD signaling, *Nat. Biotechnol.*, 2009, **27**, 275.

33 G. Lee, S. M. Chambers, M. J. Tomishima and L. Studer, Derivation of neural crest cells from human pluripotent stem cells, *Nat. Protoc.*, 2010, **5**, 688.

34 S. J. Arnold and E. J. Robertson, Making a commitment: cell lineage allocation and axis patterning in the early mouse embryo, *Nat. Rev. Mol. Cell Biol.*, 2009, **10**, 91.

35 G. M. C. Rodrigues, T. Gaj, M. M. Adil, J. Wahba, A. T. Rao, F. K. Lorbeer, R. U. Kulkarni, M. M. Diogo, J. M. S. Cabral, E. W. Miller, D. Hockemeyer and D. V. Schaffer, Defined and Scalable Differentiation of Human Oligodendrocyte Precursors from Pluripotent Stem Cells in a 3D Culture System, *Stem Cell Rep.*, 2017, **8**(6), 1770–1783.

36 J. G. Camp, F. Badsha, M. Florio, S. Kanton, T. Gerber, M. Wilsch-Brauninger, E. Lewitus, A. Sykes, W. Hevers, M. Lancaster, J. A. Knoblich, R. Lachmann, S. Paabo, W. B. Huttner and B. Treutlein, Human cerebral organoids recapitulate gene expression programs of fetal neocortex development, *Proc. Natl. Acad. Sci. U. S. A.*, 2015, **112**(51), 15672–15677.

37 C.-T. Lee, R. M. Bendriem, W. W. Wu and R.-F. Shen, 3D brain Organoids derived from pluripotent stem cells: promising experimental models for brain development and neurodegenerative disorders, *J. Biomed. Sci.*, 2017, **24**(1), 59.

38 P. Zhuang, A. X. Sun, J. An, C. K. Chua and S. Y. Chew, 3D neural tissue models: From spheroids to bioprinting, *Biomaterials*, 2018, **154**, 113–133.

39 J. A. Bagley, D. Reumann, S. Bian, J. Levi-Strauss and J. A. Knoblich, Fused cerebral organoids model interactions between brain regions, *Nat. Methods*, 2017, **14**(7), 743–751.

40 C. Fredriksson, M. Hedhammar, R. Feinstein, K. Nordling, G. Kratz, J. Johansson, F. Huss and A. Rising, Tissue Response to Subcutaneously Implanted Recombinant Spider Silk: An in Vivo Study, *Materials*, 2009, **2**(4), 1908–1922.